

Dilute nonisovalent (II-VI)-(III-V) semiconductor alloys: Monodoping, codoping, and cluster doping in ZnSe-GaAs

L. G. Wang and Alex Zunger

National Renewable Energy Laboratory, Golden, Colorado 80401, USA

(Received 28 May 2003; published 30 September 2003)

A dilute nonisovalent semiconductor alloy, made of a III-V semiconductor component (GaAs) mixed with a II-VI semiconductor (ZnSe), can be viewed as the doping of a host semiconductor with a lower (higher) valent cation and a higher (lower) valent anion. We have investigated different doping types, i.e., monodoping, triatomic codoping, and cluster doping, in the ZnSe-GaAs system using *ab initio* pseudopotential plane-wave calculations. We find the following: (i) The acceptor dopant clusters are stabilized in a chemical potential range different from that of the donor dopant clusters. This explains the experimental observation that a nonisovalent alloy has a distinct carrier polarity. (ii) Cluster doping, e.g., $(\text{Zn-Se}_4)^{3+}$ or $(\text{Se-Zn}_4)^{3-}$ in GaAs, is predicted to be stable at extreme chemical potential limits, and also to contribute free carriers. (iii) Triatomic codoping is predicted to be thermodynamically unstable. (iv) Cluster doping produces shallower acceptor/donor levels than monodoping and triatomic codoping. (v) There is a strong attractive interaction between positively charged donors and negatively charged acceptors. Therefore, a high concentration of the charge-neutral dopant pairs exists in the alloy. This finding explains why free carriers in a nonisovalent alloy have a high mobility. (vi) Our results also explain the asymmetric dependence of the band gap on the alloy composition. Specifically, adding a small amount of Ga+As into ZnSe leads to a sharp drop in the band gap of the host crystal, whereas adding Zn+Se into GaAs does not change the band gap very much.

DOI: 10.1103/PhysRevB.68.125211

PACS number(s): 61.72.Vv, 61.66.Dk, 71.15.Nc

I. INTRODUCTION: NONISOVALENT SEMICONDUCTOR ALLOYS

Conventional semiconductor alloys are isovalent, being based on mixing, e.g., III-V and III-V compounds, or II-VI and II-VI compounds. These systems tend to be electrically neutral, and with the exception of isovalent first row impurities (e.g., N in III-Vs or O in II-VIs) they do not produce any new levels in the fundamental band gap. In contrast, the simultaneous introduction of low-valent and high-valent elements into a III-V compound leads nominally to the formation of a “nonisovalent alloy,”¹⁻⁷ e.g., $(\text{GaAs})_x(\text{ZnSe})_{1-x}$. Compared with isovalent alloys that involve two semiconductors of the same material class, the nonisovalent alloys exhibit surprising phenomenology: (i) whereas the existence of both hole-producing acceptors (e.g., ZnSe:As) and electron-producing donors (e.g., ZnSe:Ga) in nonisovalent alloys was expected to lead to charge compensation,¹ surprisingly, most nonisovalent alloys exhibit *either* free electrons *or* free holes, depending on growth conditions.⁴⁻⁶ Yet (ii) carrier mobilities are surprisingly high, suggesting the existence of unspecified, charge-neutral objects within the alloys that, unlike charged centers, scatter electrons only minimally.⁷ (iii) It was found^{1,2} that whereas introduction of a smaller band gap III-V dopants into the large-gap II-VI host crystal leads to a rapid decrease of the alloy band gap, introduction of II-VI dopants into the III-V host crystal creates surprisingly but a small change in the band gap.

The aforementioned phenomenology refers to well developed, concentrated $(\text{III-V})_x(\text{II-VI})_{1-x}$ alloys. However, at

low concentration, the problem can be viewed as one of electrical doping. In the present study, we consider Zn+Se doping of GaAs, as well as Ga+As doping of ZnSe. To understand the basic building blocks of doping in such systems, we can imagine placing various X atom centered A_nB_{4-n} tetrahedral clusters with $0 \leq n \leq 4$ inside the host crystal. For the GaAs host we can consider the five Se-centered $\text{Se}-(\text{Zn}_{4-n}\text{Ga}_n)$ tetrahedra, and the five Zn-centered $\text{Zn}-(\text{Se}_{4-m}\text{As}_m)$ tetrahedra, where both n and m range $n, m = 0, 1, 2, 3, \text{ and } 4$. These tetrahedra are formed by substituting with Zn and Se atoms the five sites of a single natural As-Ga₄ or Ga-As₄ tetrahedron inside bulk GaAs crystal. In the present study we limit the dopant cluster size up to five host lattice sites. These clusters cover all elementary doping forms: *monodoping* of Se in GaAs corresponds to $n=4$ (Se-Ga₄ tetrahedron), whereas monodoping of Zn in GaAs corresponds to $m=4$ (Zn-As₄ tetrahedron). *Diatomic dopant pairs*, e.g. the Zn-Se molecule in GaAs, correspond to $n=3$ or $m=3$. *Triatomic (“co”) doping*, i.e., 2Zn+Se and Zn+2Se in GaAs, corresponds to $n=2$ and $m=2$, respectively. Finally, *cluster doping* corresponds to $n=0$ or 1 and $m=0$ or 1. Analogously, considering Ga+As doping of ZnSe, we have another ten clusters: the five Ga-centered clusters $\text{Ga-As}_{4-n}\text{Se}_n$ and the five Se-centered clusters $\text{Se-Zn}_{4-n}\text{Ga}_n$.

We have investigated the different doping types—monodoping, codoping, and cluster doping—in the GaAs-ZnSe system by *ab-initio* pseudopotential plane-wave calculations. We find that (i) codoping is thermodynamically unstable in this system, whereas “cluster doping” (e.g.,

Se-Zn₄ and Zn-Se₄ tetrahedra in GaAs) is stable and produces free carriers. We further explain the surprising phenomenology in this nonisovalent alloy: (ii) it exhibits *either* *n*-type or *p*-type behavior, rather than charge compensation; (iii) the dependence of band gap on the alloy composition is asymmetric; and (iv) free carriers have a high mobility.

II. METHOD OF CALCULATION

A. Formation enthalpy and defect transition energy

The formation enthalpy $\Delta H^{(\alpha,q)}(\mu, E_F)$ of defect α in charge state q depends on the chemical potentials μ of all species involved and on the Fermi energy E_F , and is given by

$$\Delta H^{(\alpha,q)}(\mu, E_F) = \Delta H^{(\alpha,0)}(\mu) - q\epsilon(0/q) + qE_F. \quad (1)$$

Here, $\Delta H^{(\alpha,0)}(\mu)$ is the formation enthalpy of the neutral ($q=0$) defect, and $\epsilon(0/q)$ is the defect transition energy from charge state 0 to q , *i.e.* the value of the Fermi energy where $\Delta H^{(\alpha,q)} = \Delta H^{(\alpha,0)}$. The formation energy of a neutral defect,

$$\Delta H^{(\alpha,0)} = [E_{tot}^{(\alpha,0)} - E_{tot}^{pure}] - \sum_i N_i \mu_i, \quad (2)$$

is calculated from the difference in total energy $E_{tot}^{(\alpha,0)}$ of a supercell containing defect α and a supercell of the pure host material E_{tot}^{pure} , corrected by the chemical potential term due to the transfer of N_i atoms of type i ($=$ Ga, As, Zn, Se) between the defect supercell and the chemical reservoirs with which the system is in equilibrium. The “defect transition level $\epsilon^{(\alpha)}(0/q)$ ” denotes the energy where the defect changes from being charge neutral to having a charge q ; here $q < 0$ implies an acceptor (producing holes, rendering the material *p* type), whereas $q > 0$ implies a donor (producing electrons, and rendering the material *n* type). The defect transition energy level, (which does not depend on chemical potentials),

$$\epsilon(0/q) = -\frac{1}{q} [E_{tot}^{(\alpha,q)} - E_{tot}^{(\alpha,0)} + qE_{VBM}], \quad (3)$$

is calculated from the difference in total energy of a supercell containing the defect α in charge state q , and the supercell with the neutral defect, corrected for charge neutrality by the term qE_{VBM} , where E_{VBM} is the zero of the Fermi level at the valence band maximum (VBM). Charge neutrality is affected in the calculation by placing the balance of charge in a uniform jellium background. E_{VBM} is taken from the value of the bulk host material.

Our calculations were performed using the pseudopotential plane-wave total-energy method,^{8,9} with the local density approximation (LDA) for the exchange-correlation potential.^{10,11} The Vanderbilt ultrasoft pseudopotentials,¹² which include five, six, 12, and 13 valence electrons for As, Se, Zn, and Ga, respectively, are employed to represent the interaction of the core and valence electrons for these atoms. A $4 \times 4 \times 4$ Monkhorst-Pack grid of wave vectors in the Brillouin zone of a 64-atom supercell and the plane wave basis cutoff energy of 200 eV are used in our calculations. Both

host and dopant atoms in the supercell are allowed to relax to achieve minimum energy. We tested the convergence of the formation enthalpy results with respect to the GGA (generalized gradient approximation) exchange-correlation potential,¹³ plane wave basis cutoff energy, \mathbf{k} points, and supercell size. In particular, we tested a large 216-atom supercell with the defect at its high charge state ($q = +3$ or -3) and found that the formation enthalpies are converged to an accuracy of 0.3 eV. Therefore, we did not further correct our results for charged systems due to the use of periodic boundary conditions.¹⁴

B. Chemical potential limits

The allowed chemical potential range is determined by a set of thermodynamic conditions^{15,16} that assure that competing phases [i.e., elemental solids Ga, As, Zn, and Se, and dopant associates] do not precipitate. Consider the example of Zn+Se doping of GaAs:

(i) In order to prevent formation of elemental bulks, we have

$$\mu_i - \mu_i^S \leq 0, \quad (4)$$

where $i =$ Ga, As, Zn, and Se.

(ii) For the GaAs host, we have at equilibrium

$$(\mu_{Ga} - \mu_{Ga}^S) + (\mu_{As} - \mu_{As}^S) = \Delta H_f^{GaAs}, \quad (5)$$

where ΔH_f^{GaAs} is *formation enthalpy* of GaAs.

(iii) For dopants Zn and Se in the GaAs host, we have

$$(\mu_{Zn} - \mu_{Zn}^S) + (\mu_{Se} - \mu_{Se}^S) \leq \Delta H_f^{ZnSe}. \quad (6)$$

An alternative form of Eq. (6) is

$$(\mu_{Zn} - \mu_{Zn}^S) + (\mu_{Se} - \mu_{Se}^S) = \Delta H_f^{ZnSe} + K, \quad (7)$$

where ΔH_f^{ZnSe} is *formation enthalpy* of ZnSe, and $K \leq 0$.

(iv) In order to prevent the formation of Zn₃As₂ precipitates, we require

$$3(\mu_{Zn} - \mu_{Zn}^S) + 2(\mu_{As} - \mu_{As}^S) \leq \Delta H_f^{Zn_3As_2}. \quad (8)$$

(v) In order to prevent the formation of Ga₂Se₃ precipitates, we require

$$2(\mu_{Ga} - \mu_{Ga}^S) + 3(\mu_{Se} - \mu_{Se}^S) \leq \Delta H_f^{Ga_2Se_3}. \quad (9)$$

μ_i^S in Eqs. (4)–(9) are the chemical potential of the elemental solids. When $K < 0$ the dopants tend to exist in the host crystal as isolated atoms (“dilute dopant sources”), whereas when $K \sim 0$ the dopants tend to form aggregates (“concentrated dopant sources”). The dopant chemical potential can be adjusted by controlling the dopant sources, e.g. by using concentrated or dilute dopant sources. As to the lower bound on K , we estimate from the solubility of Zn and Se in GaAs that $K \geq -1$ eV (see Ref. 16). Our LDA total energy calculations give -0.65 , -1.36 , -2.4 , and -0.39 eV for ΔH_f^{GaAs} , ΔH_f^{ZnSe} , $\Delta H_f^{Ga_2Se_3}$, and $\Delta H_f^{Zn_3As_2}$, respectively. The allowed chemical potential ranges determined by Eqs. (4)–(9) are shown in Fig. 1. We obtain for Zn+Se doping of

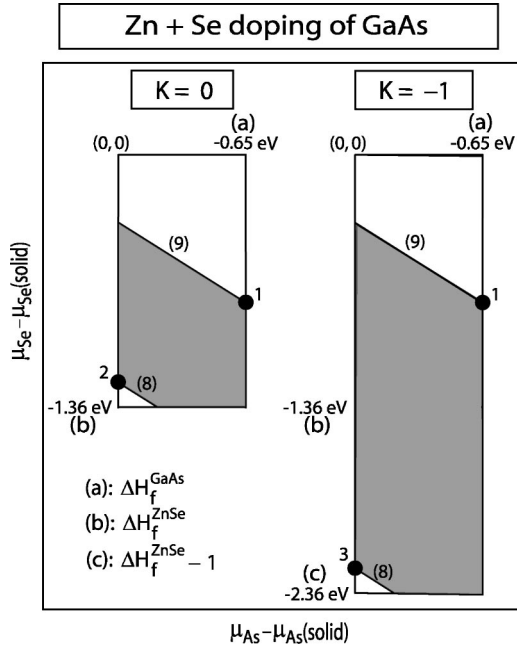


FIG. 1. The allowed chemical potential ranges for Zn+Se doping of GaAs given by the shaded regions. Points 1 and 2 determine the lower and upper limits of the chemical potential difference $\mu_{As} - \mu_{Se}$ for $K=0$, and points 1 and 3 determine the lower and upper limits of the chemical potential difference $\mu_{As} - \mu_{Se}$ for $K = -1$. Lines (8) and (9) correspond to Eqs. (8) and (9), respectively.

GaAs $-1.078 \leq \mu_{As} - \mu_{Se} \leq 0.002$ eV for $K=0$ and $-1.078 \leq \mu_{As} - \mu_{Se} \leq 1.002$ for $K=-1$ eV. For Ga+As doping of ZnSe, we can perform a similar analysis. The allowed chemical potential ranges are shown in Fig. 2. We obtain $-1.078 \leq \mu_{As} - \mu_{Se} \leq 0.002$ eV for $K=0$, and

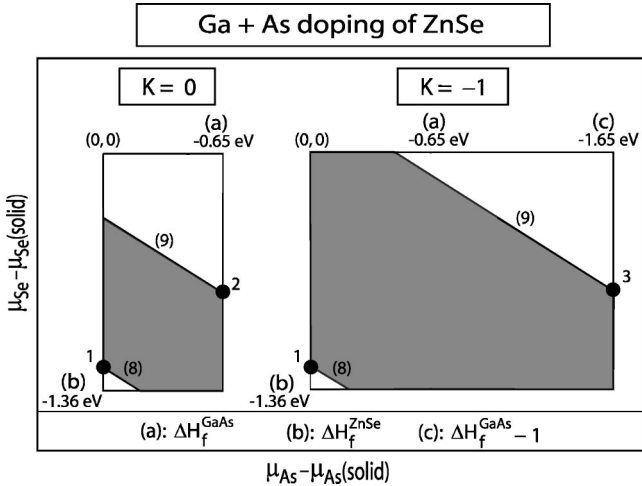


FIG. 2. The allowed chemical potential ranges for Ga+As doping of ZnSe given by the shaded regions. Points 1 and 2 determine the upper and lower limits of the chemical potential difference $\mu_{As} - \mu_{Se}$ for $K=0$, and points 1 and 3 determine the upper and lower limits of the chemical potential difference $\mu_{As} - \mu_{Se}$ for $K = -1$. Lines (8) and (9) correspond to Eqs. (8) and (9), respectively.

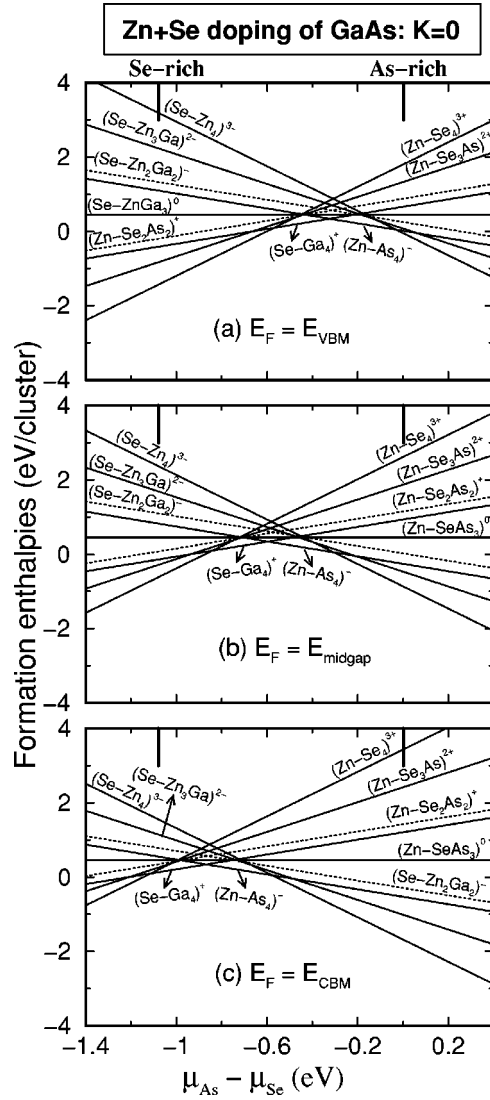


FIG. 3. Formation enthalpies of Zn+Se dopants in GaAs for $K=0$ with the Fermi energy at (a) $E_F = E_{VBM}$, (b) $E_F = E_{midgap}$, and (c) $E_F = E_{CBM}$. Triatomic codoping is shown by dashed lines. The vertical bars indicate the allowed chemical potential range of $\mu_{As} - \mu_{Se}$.

$-2.078 \leq \mu_{As} - \mu_{Se} \leq 0.002$ for $K=-1$ eV. We will thus compare different forms of doping in these allowed ranges of chemical potentials.

III. DOPING GaAs BY Zn+Se AND DOPING ZnSe BY Ga+As

Figure 3 shows the formation enthalpy results for Zn+Se doping of GaAs, and Fig. 4 shows the same results for Ga+As doping of ZnSe. The results are given for rich dopant concentration ($K=0$) and at three values of E_F (a) $E_F = E_{VBM}$, (b) $E_F = E_{midgap}$, and (c) $E_F = E_{CBM}$. For the case (b) we also explore for dilute dopant concentration ($K = -1$ eV) in Fig. 5.

Table I shows the calculated bond lengths of Zn-centered and Se-centered clusters in GaAs. We see, relative to the

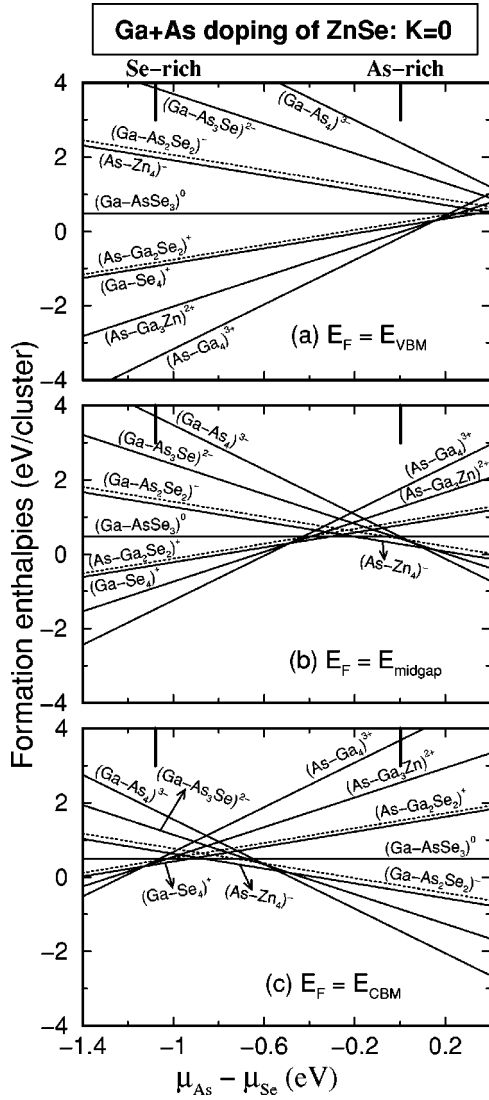


FIG. 4. Formation enthalpies of Ga+As dopants in ZnSe for $K=0$ with the Fermi energy at (a) $E_F=E_{VBM}$, (b) $E_F=E_{midgap}$, and (c) $E_F=E_{CBM}$. Triatomic codoping is shown by dashed lines. The vertical bars indicate the allowed chemical potential range of $\mu_{As}-\mu_{Se}$.

bulk, that the Zn-Se bond length increases in the GaAs environment, and this increase is greater the more As exists in the $Zn-Se_{4-n}As_n$ clusters. The same is true for the Zn-Se bond in the Se-centered clusters $Se-Zn_{4-n}Ga_n$, where the bond increases with increasing Ga content in the cluster. Table II shows analogous results for the Ga-centered $Ga-As_{4-n}Se_n$ cluster in ZnSe and the As-centered cluster $As-Ga_{4-n}Zn_n$ in ZnSe.

A. Formation enthalpies for p -type doping of GaAs by Zn+Se

For p -type doping we need to look at the formation enthalpies of various dopant clusters for the Fermi energy close to the VBM. Figure 3(a) shows the formation enthalpy results for Zn+Se doping of GaAs at $E_F=E_{VBM}$. We see that (i) under maximally As-rich conditions, cluster doping [(Se-Zn₄)³⁻ and (Se-Zn₃Ga)²⁻] and monodoping of Zn

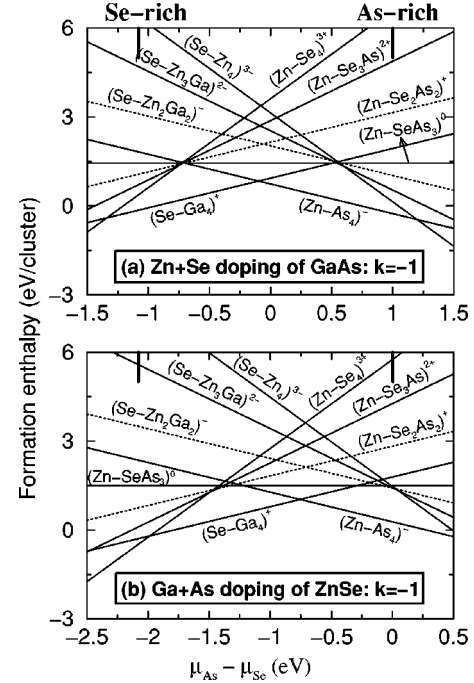


FIG. 5. Formation enthalpies for dilute dopant sources $K=-1$ with the Fermi energy at $E_F=E_{midgap}$: (a) Zn and Se doping of GaAs; (b) Ga and As doping of ZnSe. Triatomic codoping is shown by dashed lines. The vertical bars indicate the allowed chemical potential range of $\mu_{As}-\mu_{Se}$.

[denoted as $(Zn-As_4)^-$], which both promote p -type conductivity, have lower formation enthalpies than the donor dopant clusters. We thus predict that the above dopant clusters can form in nonisovalent ZnSe-GaAs alloys and produce free holes. Although the acceptor codoping [(Se-Zn₂Ga)⁻] is never the ground state, its formation energy is low and, therefore, it could have a considerable concentration in the alloy. (ii) For the intermediate chemical potential range up to the maximally Se-rich limit, the donor dopant clusters [clus-

TABLE I. Calculated bond lengths for Zn-centered dopant clusters $Zn-Se_{4-n}As_n$ and Se-centered dopant clusters $Se-Zn_{4-n}Ga_n$ in GaAs. The theoretical Zn-Se bond length in ZnSe is 2.42 Å.

| Zn-centered dopant clusters | | |
|------------------------------------|----------------|----------------|
| | Zn-As bond (Å) | Zn-Se bond (Å) |
| Zn-As ₄ | 2.40 | |
| Zn-SeAs ₃ | 2.39 | 2.51 |
| Zn-Se ₂ As ₂ | 2.38 | 2.49 |
| Zn-Se ₃ As | 2.37 | 2.46 |
| Zn-Se ₄ | | 2.44 |
| Se-centered dopant clusters | | |
| | Ga-Se bond (Å) | Zn-Se bond (Å) |
| Se-Ga ₄ | 2.52 | |
| Se-ZnGa ₃ | 2.50 | 2.51 |
| Se-Zn ₂ Ga ₂ | 2.46 | 2.48 |
| Se-Zn ₃ Ga | 2.43 | 2.45 |
| Se-Zn ₄ | | 2.42 |

TABLE II. Calculated bond lengths for Ga-centered dopant clusters $\text{Ga-As}_{4-n}\text{Se}_n$ and As-centered dopant clusters $\text{As-Ga}_{4-n}\text{Zn}_n$ in ZnSe. The theoretical Ga-As bond length in ZnSe is 2.43 Å.

| Ga-centered dopant clusters | | |
|------------------------------------|----------------|----------------|
| | Ga-Se bond (Å) | Ga-As bond (Å) |
| Zn-As ₄ | 2.48 | |
| Zn-SeAs ₃ | 2.45 | 2.35 |
| Zn-Se ₂ As ₂ | 2.47 | 2.37 |
| Zn-Se ₃ As | 2.48 | 2.40 |
| Zn-Se ₄ | | 2.42 |
| As-centered dopant clusters | | |
| | Zn-As bond (Å) | Ga-As bond (Å) |
| Se-Ga ₄ | 2.36 | |
| Se-ZnGa ₃ | 2.36 | 2.35 |
| Se-Zn ₂ Ga ₂ | 2.38 | 2.38 |
| Se-Zn ₃ Ga | 2.39 | 2.41 |
| Se-Zn ₄ | | 2.44 |

ter doping $(\text{Zn-Se}_4)^{3-}$ and $(\text{Zn-Se}_3\text{As})^{2-}$, monodoping of Se (denoted as $(\text{Se-Ga}_4)^+$), and codoping $(\text{Zn-Se}_2\text{As}_2)^-$, which promote an n -type behavior, have lower formation enthalpies than the acceptor dopant clusters. Actually, the formation enthalpies of the donor dopant clusters are negative under Se-rich conditions, which means that the donor dopant clusters can reach a very high concentration, even higher than the available sites, if the dopants are available. These donor dopant clusters, which generate free electrons, tend to compensate the p -type doping. Therefore, it is necessary to keep As-rich conditions in order to obtain a p -type doping.

The formation enthalpy depends linearly on the Fermi energy [see Eq. (1)]. When the Fermi energy is shifted to the middle of the gap, there is a larger chemical potential range for which the acceptor dopant clusters are more stable than the donor dopant clusters are [see Fig. 3(b) for $E_F = E_{midgap}$].

B. Formation enthalpies for n -type doping of GaAs by Zn+Se

To achieve n -type doping, we need to consider the formation enthalpies of various dopant clusters for the Fermi energy close to the conduction band minimum (CBM). Figure 3(c) shows the results for Zn+Se doping of GaAs at the Fermi energy $E_F = E_{CBM}$. We see that (i) under very Se-rich conditions, the donor dopant clusters [cluster doping $(\text{Zn-Se}_4)^{3+}$ and $(\text{Zn-Se}_3\text{As})^{2+}$] and monodoping of Se [denoted as $(\text{Se-Ga}_4)^+$] have lower formation enthalpies than the acceptor dopant clusters. These dopant clusters and monodoping of Se produce free electrons and make the material n type. Again, codoping $(\text{Se-Ga}_4)^+$ is never the ground state, but has a low formation enthalpy at the very Se-rich limit and can thus result in a considerable concentration in the alloy. (ii) For the intermediate chemical potential range up to the very As-rich limit, the acceptor dopant clusters [such as monodoping of Zn and cluster doping $(\text{Se-Zn}_4)^{3-}$ and $(\text{Se-Zn}_3\text{Ga})^{2-}$] become more stable than the donor dopant

clusters and tend to compensate the n -type doping. Therefore, in order to obtain n -type doping it is necessary to keep Se-rich conditions.

When the Fermi energy is shifted to the middle of the gap, there is a larger chemical potential range for which the donor dopant-clusters are more stable than the acceptor dopant-clusters are [see Fig. 3(b) for $E_F = E_{midgap}$]. This indicates a self-regulating effect of doping: When the Fermi energy is located at the middle of the gap (as is the case for a material that is undoped or is lightly doped), it is possible to form either acceptor or donor centers; however, when the Fermi energy is moved towards the VBM (by external p -type doping) it becomes more difficult to introduce acceptor defects. Conversely, when the Fermi energy is moved towards the CBM (by external n -type doping) it becomes more difficult to introduce donor defects. We conclude that doping GaAs by Zn+Se is done most effectively via *cluster doping*, both for “As-rich p -type” conditions and “Se-rich n type” conditions.

C. Formation enthalpies for p -type doping of ZnSe by Ga+As

Figure 4(a) shows the formation enthalpies for Ga+As doping of ZnSe at the Fermi energy $E_F = E_{VBM}$. We see that for the entire allowed chemical potential range the donor dopant clusters [including cluster-doping $(\text{As-Ga}_4)^{3+}$ and $(\text{As-Ga}_3\text{Zn})^{2+}$, monodoping of Ga, and codoping $(\text{As-Ga}_2\text{Zn}_2)^+$] have lower formation enthalpies than the acceptor dopant clusters, i.e., cluster doping $(\text{Ga-As}_4)^{3-}$, and $(\text{Ga-As}_3\text{Se})^{2-}$, codoping $(\text{Ga-As}_2\text{Se}_2)^-$, and monodoping of As. Therefore, in this case p -type doping is defeated. This is consistent with the experimental observation that it is difficult to dope ZnSe p type,¹⁷ and is opposite to the case of p -type doping of GaAs by Zn+Se [Fig. 3(a)], where there is a chemical potential range that p -type doping is possible.

If the Fermi energy is shifted to the middle of the gap (which is possible when the material is undoped or is slightly doped), it is favorable to form acceptor dopant clusters. Figure 4(b) shows the results when the Fermi energy $E_F = E_{midgap}$. We see that (i) under very As-rich conditions, the acceptor dopant-clusters [monodoping of As, cluster doping $(\text{Ga-As}_4)^{3-}$ and $(\text{Ga-As}_3\text{Se})^{2-}$ and codoping $(\text{Ga-As}_2\text{Se}_2)^-$] are more stable than the donor dopant clusters are. Therefore, these acceptor dopant clusters contribute free holes under very As-rich conditions with the Fermi energy close to the middle gap. (ii) Under Se-rich conditions, the donor dopant clusters are more stable than the acceptor dopant clusters are. These donor dopant clusters generate free electrons and tend to compensate the hole-producing acceptor centers or make the material n type.

D. Formation enthalpies for n -type doping of ZnSe by Ga+As

Figure 4(c) shows the formation enthalpy results for Ga+As doping of ZnSe at the Fermi energy $E_F = E_{CBM}$. Similar to the Zn+Se doping of GaAs, we see that (i) under maximally Se-rich conditions, the donor dopant clusters are more stable than the acceptor dopant-clusters are. These donor dopant clusters [cluster doping $(\text{As-Ga}_4)^{3+}$ and $(\text{As-Ga}_3\text{Zn})^{2+}$, codoping $(\text{As-Ga}_2\text{Zn}_2)^+$, and mono-

TABLE III. Ground state structures determined from formation enthalpy calculations for various Fermi energies under Se-rich or As-rich conditions.

| | $E_F = E_{VBM}$ | $E_F = E_g/2$ | $E_F = E_{CBM}$ |
|----------------------|-------------------------|-------------------------|-------------------------|
| Zn+Se doping of GaAs | | | |
| Se rich | $(\text{Zn-Se}_4)^{3+}$ | $(\text{Zn-Se}_4)^{3+}$ | $(\text{Se-Ga}_4)^+$ |
| As rich | $(\text{Se-Zn}_4)^{3-}$ | $(\text{Se-Zn}_4)^{3-}$ | $(\text{Se-Zn}_4)^{3-}$ |
| Ga+As doping of ZnSe | | | |
| Se rich | $(\text{As-Ga}_4)^{3+}$ | $(\text{As-Ga}_4)^{3+}$ | $(\text{Ga-Se}_4)^+$ |
| As rich | $(\text{As-Ga}_4)^{3+}$ | $(\text{As-Zn}_4)^-$ | $(\text{Ga-As}_4)^{3-}$ |

doping of Ga] generate free electrons and promote n -type doping. (ii) From the intermediate chemical potential range to the very As-rich limit, the acceptor dopant clusters [cluster doping $(\text{Ga-As}_4)^{3-}$ and $(\text{Ga-As}_3\text{Se})^{2-}$, codoping $(\text{Ga-As}_2\text{Se}_2)^-$, and monodoping of As] have lower formation enthalpies than the donor dopant-clusters, which means a strong compensation to n -type doping for this chemical potential range. So in order to obtain n -type doping it is necessary to keep very Se-rich conditions.

Again, we see that when the Fermi energy is shifted from the CBM to the middle of the gap, the chemical potential range for which the donor dopant clusters are more stable than the acceptor dopant clusters is increased [see Fig. 4(b) for $E_F = E_{midgap}$]. Therefore, it is favorable to form donor dopant-clusters at the Fermi energy $E_F = E_{midgap}$.

We conclude that doping ZnSe by Ga+As is done most effectively by *cluster doping* for “Se-rich n -type” conditions, whereas cluster doping can promote p -type doping only when E_F is close to the middle gap.

E. Dilute vs concentrated dopant sources

Figure 5 shows the formation enthalpy results for dilute dopant concentration ($K = -1$ eV). We see that dilute dopant sources broaden considerably the stability range of monodoping: We predict that the rather narrow stability domains of monodoping in GaAs and ZnSe attainable under *concentrated* dopant sources [see Figs. 3(b) and 4(b)] will considerably broaden using *dilute* dopant sources (Fig. 5). Thus, dilute dopant sources favor monodoping. This observation shows that the behavior of dopants in alloys can be controlled by adjusting dopant sources, and further suggests that p -type doping of ZnSe can be facilitated by use of dilute sources.

IV. GENERAL PROPERTIES OF DILUTE NONISOVALENT ALLOYS

A. Distinct carrier polarity

It was once thought¹ that alloying of a semiconductor such as GaAs by a semiconductor having both a lower-valent cation (Zn) and a higher-valent anion (Se) will lead to charge compensation, whereby the Zn_{Ga} acceptor will negate the Se_{As} donor. In contrast, we find that *electron*-producing

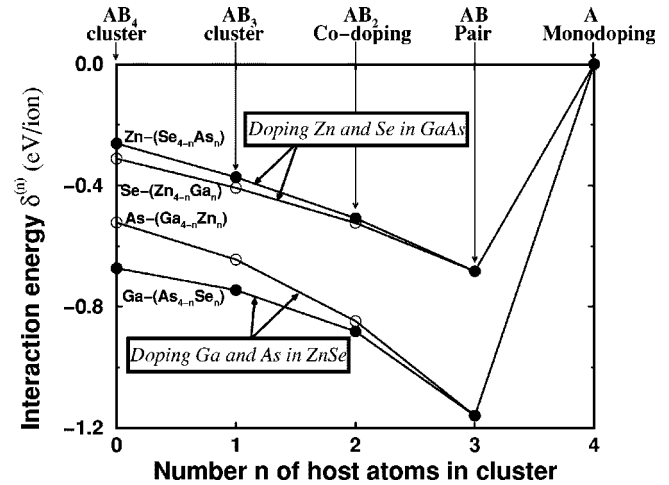


FIG. 6. The energy of a dopant cluster $X-(A_{4-n}B_n)$ relative to the energies of isolated dopants plotted against the cluster type n , including monodoping ($n=4$), pairs ($n=3$), codoping ($n=2$), and cluster doping ($n=1,0$).

mono-doping is stable in a different range of chemical potentials than *hole*-producing mono-doping, so the alloy has a definite charge polarity, as seen experimentally.⁴⁻⁶ At some critical chemical potential $\mu_{\text{As}} - \mu_{\text{Se}}$ shown in Figs. 3–5 as the boundary between the two monodoping regions, we predict a transition between the two polarities. Table III summarizes the stable clusters at different $\mu_{\text{As}} - \mu_{\text{Se}}$. The reason for the existence of distinct alloy polarities is that at the same chemical potential the solubility of anions generally differs from that of cations. For example, at the As-rich limit of Fig. 5(a) monodoping of Zn in GaAs has a formation energy of -0.26 eV, whereas for same conditions, monodoping of Se has a formation energy of 1.94 eV.

We see from Figs. 3 and 4 and Table III that the well-known trend that if $E_F = E_{VBM}$ (p -type sample) then the *donor* dopant clusters are easily stabilized, whereas if $E_F = E_{CBM}$ (n -type sample) then the *acceptor* dopant clusters are easily stabilized. However, there are exceptions: under As-rich conditions one could create acceptors even in p -type GaAs, and under Se-rich conditions one can create donors even in n -type GaAs. These trends are weaker in ZnSe: it is difficult to create acceptors in p -type ZnSe even under As-rich conditions, but if $E_F = E_{midgap}$, one can create acceptors in ZnSe under As-rich conditions.

B. Existence of dopant pairs

We have calculated the interaction energy $\delta^{(n)}$ between the components of a dopant cluster, i.e., the energy difference between a dopant cluster and infinitely separated component dopants in the cluster. For example, $\delta^{(3)}$ is the energy of a Zn-Se diatomic pair in GaAs relative to monodoping of Zn (Zn-As_4) plus monodoping of Se (Se-Ga_4). Figure 6 shows the interaction energies $\delta^{(n)}$ for the four families of clusters. We find that association of dopants lowers the energy ($\delta < 0$), especially for the dopant *pairs* Ga-As in ZnSe and Zn-Se in GaAs. This attractive interaction between op-

positively charged isolated dopants leads to a minimum in $\delta^{(n)}$ for pairs, and implies that a significant concentration of dopant pairs will exist in such alloys. The charge neutrality of such pairs may explain the surprisingly high carrier mobility⁷ in nonisovalent alloys in terms of weak dipolar (rather than charged-ion) scattering. Note that neutral clusters ($n=3$) do not contribute to doping, whereas charged clusters (e.g. $n=4$ and 0) which contribute to doping also contribute to enhance scattering.

The greater tendency for clustering of the small gap Ga+As in ZnSe than for the large-gap Zn+Se in GaAs (Fig. 6) may also explain the fact^{1,2} that dissolving Ga+As in ZnSe leads to the creation of a smaller band gap, akin to GaAs-like clusters, while dissolving Zn+Se in GaAs does not change the host crystal band gap.

C. Thermodynamic instability of codoping

The formation enthalpies of triatomic co-doping are shown in Figs. 3 and 4 by dashed lines. We see that the p -type codoping $(\text{Se-Zn}_2\text{Ga}_2)^-$ and the n -type codoping $(\text{Zn-Se}_2\text{As}_2)^+$ in GaAs are never the ground state structures for any value of (μ, E_F) . The same is true for the n -type codoping $(\text{As-Ga}_2\text{Zn}_2)^+$ and the p -type codoping $(\text{Ga-As}_2\text{Se}_2)^-$ in ZnSe (Fig. 4). Codoping becomes even less favorable when using dilute dopant sources (see Fig. 5). Thus, if codoping is the dominating form of doping in this system,¹⁸⁻²² it is not mandated by thermodynamics. This conclusion focuses attention on the possibility of nonequilibrium metastable species, since stable species do not lead here to codoping.²³ The instability of codoping reflects the balance of two competing interactions.²⁴ In p -type codoping we have two acceptors and one donor; we find that the repulsive acceptor-acceptor interaction overwhelms the attractive donor-acceptor interaction, resulting in a lower stability relative to monodoping.

D. Thermodynamic stability of cluster-doping

Unlike triatomic codoping which is unstable, some tetrahedral pure-dopant clusters are predicted to be thermodynamically stable (see Figs. 3 and 4 and Table III). Figure 3 shows, for example, that in GaAs the Zn-Se₄ cluster is the stablest structure under Se-rich conditions, whereas Se-Zn₄ is the stablest structure under As-rich conditions for dopant rich sources ($K=0$). These dopant clusters are stabilized under extreme chemical potentials because of the stronger dependence of their formation enthalpies on the chemical potential (see Figs. 3 and 4 the corresponding slopes). We estimate that the configurational entropy contribution at room temperature is about 0.2 eV in favor of stabilizing the monodoping (the vibrational entropy has even a much smaller contribution). But ignoring the entropy contributions as we have done in the present study will not affect our conclusion that the cluster doping can be stabilized under extreme chemical potentials. The predicted thermodynamic stability and carrier production of tetrahedral clusters in GaAs and ZnSe implies that the ratio between incorporated cation and anion dopants will not be 2:1 (as in the proposed¹⁸

n -type codoping of GaAs by Zn+2Se), but rather higher, e.g., Zn+4Se n doping in GaAs. So cluster doping may be realized in experiments by working with a high (3:1 or 4:1) ratio of acceptor-to-donor for p -type doping (and a high ratio of donor-to-acceptor in n -type doping), and pushing the chemical potential conditions to the extreme limits.

Cluster doping may also prevent a spontaneous, symmetry-lowering deformation, turning a shallow defect into a deep one.²⁵ This is because in the tetrahedral pure-dopant clusters the bonds satisfy, at least locally, the octet rule.

E. Shallower acceptor/donor transition levels by cluster doping

For doping ionizability is an important factor which should be considered. As pointed out in Sec. II, the defect transition energy does not depend on the chemical potentials. Our results indicate that cluster doping generates a shallower level than monodoping and triatomic codoping. For p -type doping in GaAs, triatomic codoping $(\text{Se-Zn}_2\text{Ga}_2)^-$ has an acceptor level $[\epsilon(0/-)]$ which is 12 meV shallower than monodoping of Zn, and the acceptor level $[\epsilon(0/-)]$ of cluster doping $(\text{Se-Zn}_4)^-$ is 261 meV shallower than the acceptor level of the codoping. For n -type doping in GaAs, we find that the donor level $[\epsilon(0/+)]$ of codoping $(\text{Zn-Se}_2\text{As}_2)^+$ is 71 meV shallower than monodoping of Se, and the cluster doping $(\text{Zn-Se}_4)^+$ has a donor level $[\epsilon(0/+)]$ which is shallower by 349 meV compared with codoping $(\text{Zn-Se}_2\text{As}_2)^+$. For Ga and As doping of ZnSe, we find a similar trend as in Zn and Se doping of GaAs. These results may be understood by the hybridization and level repulsion between the donor and acceptor levels.²⁶

V. CONCLUSIONS

We have performed extensive first-principles calculations for Zn+Se doping of GaAs and Ga+As doping of ZnSe. The formation enthalpies and defect transition energies are obtained for various doping types, i.e. monodoping, codoping and cluster doping. Our study clarifies the peculiar features of nonisovalent covalent alloys and general doping characteristics: (i) Covalent alloys exhibit an asymmetry between anion and cation incorporation energies, thus the alloy has a definite charge polarity. (ii) The impurities form stable but charge neutral pairs, so scattering is rather small. (iii) The greater propensity for clustering of Ga+As in ZnSe than Zn+Se in GaAs explains the larger changes in band gap in the former case. (iv) Significantly, formation of triatomic (“codoping”) molecules is thermodynamically unstable relative to monodoping, whereas cluster doping is favored. This implies an interesting principle for enhancing (cluster) doping via use of dopant-rich sources and extreme (Se-rich or As-rich) chemical potentials.

ACKNOWLEDGMENTS

This work was supported by U. S. DOE, Office of Science, DMS.

- ¹M. Glicksman and W.D. Kraeft, *Solid-State Electron.* **28**, 151 (1985).
- ²S. Bloom, *J. Appl. Phys.* **41**, 1864 (1970).
- ³M. Funato, S. Fujita, and S. Fujita, *Phys. Rev. B* **60**, 16652 (1999).
- ⁴W.M. Yim, *J. Appl. Phys.* **40**, 2617 (1969).
- ⁵A.V. Voitsekhovskii, N.G. Vyalyi, and A.D. Pashun, *Izv. Akad. Nauk SSSR, Neorg. Mater* **16**, 1909 (1980) [*Inorg. Mater. (Transl. of Neorg. Mater.)* **16**, 137 (1980)].
- ⁶N.A. Borisov, V.M. Lakeenkov, M.G. Mil'vidskii, and O.V. Pelevin, *Fiz. Tekh. Poluprovodn.* **10**, 1594 (1976) [*Sov. Phys. Semicond.* **10**, 948 (1976)].
- ⁷M. Glicksman, D. Gutman, and W.M. Yim, *Appl. Phys. Lett.* **16**, 366 (1970).
- ⁸J. Ihm, A. Zunger, and M.L. Cohen, *J. Phys. C* **12**, 4409 (1979).
- ⁹G. Kresse and J. Furthmüller, *Comput. Mater. Sci.* **6**, 15 (1996).
- ¹⁰D.M. Ceperley and B.J. Alder, *Phys. Rev. Lett.* **45**, 566 (1980).
- ¹¹J.P. Perdew and A. Zunger, *Phys. Rev. B* **23**, 5048 (1981).
- ¹²D. Vanderbilt, *Phys. Rev. B* **41**, 7892 (1990).
- ¹³J. P. Perdew, in *Electronic Structure of Solids '91*, edited by P. Ziesche and H. Eschring (Akademie-Verlag, Berlin, 1991); J.P. Perdew *et al.* *Phys. Rev. B* **46**, 6671 (1992).
- ¹⁴G. Makov and M.C. Payne, *Phys. Rev. B* **51**, 4014 (1995).
- ¹⁵S.B. Zhang and J.E. Northup, *Phys. Rev. Lett.* **67**, 2339 (1991).
- ¹⁶N.V. Karyakin and V.B. Fedoseev, *Fiz. Met. Metalloved.* **91**, 22 (2001) [*Phys. Met. Metallogr.* **91**, 126 (2001)].
- ¹⁷G.F. Neumark, *Mater. Sci. Eng., R* **R21**, 1 (1997).
- ¹⁸H. Katayama-Yoshida and T. Yamamoto, *Phys. Status Solidi B* **202**, 763 (1997).
- ¹⁹K.H. Ploog and O. Brandt, *J. Vac. Sci. Technol. A* **16**, 1609 (1998).
- ²⁰M. Joseph, H. Tabata, and T. Kawai, *Jpn. J. Appl. Phys.* **38**, L1205 (1999).
- ²¹R.Y. Korotkov, J.M. Gregie, and B.W. Wessels, *Appl. Phys. Lett.* **78**, 222 (2001).
- ²²H.D. Jung *et al.* *Appl. Phys. Lett.* **70**, 1143 (1997).
- ²³L. G. Wang and A. Zunger, *Phys. Rev. Lett.* **90**, 256401 (2003).
- ²⁴S.B. Zhang, S.H. Wei, and Y. Yan, *Physica B* **302–303**, 135 (2001).
- ²⁵D.J. Chadi, *Appl. Phys. Lett.* **59**, 3589 (1991).
- ²⁶T. Yamamoto and H. Katayama-Yoshida, *Jpn. J. Appl. Phys.* **38**, L166 (1999); *J. Cryst. Growth* **214–215**, 552 (2000); *Physica B* **302–303**, 155 (2001).